ICARUS **119,** 427–446 (1996)
ARTICLE NO. 0028

Accretion of the Moon from an Impact-Generated Disk

ROBIN M. CANUP AND LARRY W. ESPOSITO

Laboratory for Atmospheric and Space Physics, University of Colorado, Box 392, Boulder, Colorado 80309-0392
E-mail: canup@sargon.colorado.edu

Received June 9, 1995; accepted October 6, 1995

We present the first published numerical calculations of accretion of an impact-generated protolunar disk into a single large Moon. Our calculations are based on the model developed by R. M. Canup and L. W. Esposito (*Icarus* 113, 331–352, 1995) to describe accretion in the Roche zones around the giant planets. Previous numerical simulations of a large impact event predict the formation of a disk of material centered near or within the Roche limit ($\sim 2.9R_\oplus$). A natural expectation based on our previous results and comparison with the satellite systems of the outer planets would be for multiple small moons to arise from such a protolunar disk. Multiple moonlets could accrete to form a single Moon if they evolved into crossing orbits due to tidal interaction with the Earth. This would occur if the innermost moonlet in the disk were also the most massive, so that it evolved outward at the relatively fastest rate and swept up all exterior material. Our calculations, which include both moonlet accretion and orbital evolution, demonstrate that forming massive moonlets in the inner disk near the Roche limit is extremely difficult. We conclude that an Earth system with multiple moons is the final result unless some particularly severe constraints on initial conditions in the disk are met. A disk with a lunar mass of material exterior to $a \sim 3.5$–$4R_\oplus$ or an extremely steep radial surface density profile at the onset of collisional growth is required for a single, lunar-sized body to result from accretion of silicate density material in a protolunar disk. The former corresponds most closely to disks produced by impactors with nearly twice the mass of Mars and about twice the angular momentum of the current Earth/Moon system. Other processes, such as gravitational instability or primary accretion of an iron core in the inner disk, might be able to "seed" accretional growth and allow for the formation of a single Moon if disk temperature and compositional requirements are met. Our analysis demonstrates the need for more detailed, higher resolution impact simulations.

I. INTRODUCTION

The "Giant-Impact" scenario proposes that the impact of a Mars-sized protoplanet with early Earth ejected enough material into Earth orbit to form the Moon (Hartmann and Davis 1975, Cameron and Ward 1976). The impact scenario has become the favored explanation for lunar origin in the past decade, as it can potentially account for all of the major geochemical and dynamical characteristics of the Earth/Moon system: the system's high angular momentum, the depletion of volatiles in lunar material, the bulk similarity of lunar material to pre-differentiated mantle, lunar iron depletion, and lunar density. On a more fundamental level, this scenario reflects an emerging view that the final stages of Solar System formation were greatly influenced by stochastic, large impact events, the specifics of which shaped the character of the Solar System. In addition to their possible role in the formation of the Moon, large impacts may also have been responsible for the uranian 98° obliquity, the loss of mercurian mantle material, and the retrograde rotation of Venus.

Several groups of workers have conducted detailed simulations of the impact of a Mars-sized body with early Earth and have demonstrated the plausibility of formation of a protolunar disk following a large impact event. A common element to all of their results is an average semi-major axis for material ejected into bound orbits at or interior to the classical Roche limit for lunar densities ($\sim 2.9R_\oplus$).

Kipp and Melosh (1986, 1987), whose results have unfortunately been published only in preliminary forms, utilized a three-dimensional hydrocode with cell sizes ~ 250 km^2 with equations of state for dunite and iron to represent the mantles and cores of Earth and a pre-differentiated impacting body. The main limitations of their work were the neglect of self-gravity among ejected debris, and the limited amount of time after the impact which can be tracked by their finite grid map, which is only about $4R_\oplus$ in width. Kipp and Melosh (1987) found that the impact of a Mars-sized body causes ejection of a dense, hot plume of vapor which is jetted from the impact site, as well as melting of the Earth's mantle. The plume is 90% vapor and 10% liquid by mass, and has central temperatures of ~ 5500 K and pressures of 600 to 700 bar.

Benz *et al.* (1986, 1987, 1989), Cameron and Benz (1991), and Cameron (1994) have modeled giant impacts with the Earth using a smoothed-particle hydrodynamics (SPH)

0019-1035/96 $18.00

TABLE I
Impact Simulation Data

			$a < a_{Roche}$			$a > a_{Roche}$		
Target	Impactor	A.M.	Fe	Si	Total	Fe	Si	Total
2648	360	1.13	0	38	38	0	32	32
2648	360	1.17	3	33	36	0	20	20
2648	360	1.26	10	15	25	1	23	24
2648	360	1.36	2	4	6	14	36	50
2648	360	1.13	0	36	36	0	15	15
2648	360	1.25	7	15	22	2	38	40
2648	360	1.36	3	10	13	5	36	41
2648	360	1.47	0	0	0	0	0	0
2648	360	1.13	1	20	21	0	4	4
2648	360	1.25	4	15	19	0	2	2
2648	360	1.36	0	17	17	1	13	14
2593	415	1.13	0	39	39	0	3	3
2593	415	1.19	0	43	43	0	16	16
2593	415	1.24	1	27	28	0	30	30
2593	415	1.24	0	30	30	0	36	36
2593	415	1.30	0	12	12	0	40	40
2593	415	1.36	0	38	38	0	10	10
2593	415	1.47	2	36	38	3	25	28
2593	415	1.13	0	11	11	0	0	0
2593	415	1.25	0	33	33	0	5	5
2593	415	1.36	0	32	32	0	28	28
2593	415	1.47	5	36	41	0	24	24
2593	415	1.59	0	5	5	0	0	0
2593	415	1.13	0	8	8	0	0	0
2593	415	1.25	0	5	5	0	6	6
2593	415	1.36	0	35	35	0	16	16
2593	415	1.47	0	18	18	0	10	10
2593	415	1.59	0	3	3	0	0	0
2406	602	1.47	0	29	29	0	13	13
2406	602	1.59	0	41	41	0	32	32
2406	602	1.70	1	46	47	0	34	34
2406	602	1.84	10	52	62	2	44	46
2406	602	1.93	20	72	92	0	54	54
2406	602	1.59	0	60	60	0	16	16
2406	602	1.70	0	31	31	0	64	64
2406	602	1.81	1	25	26	2	44	46
2406	602	1.93	4	22	26	1	73	74
2406	602	1.59	0	34	34	0	17	17
2406	602	1.70	0	32	32	0	32	32
2406	602	1.81	0	9	9	1	44	45
2406	602	1.93	1	34	35	0	48	48

Note. Data from Cameron and Benz (1991). All integers are particle numbers, with a lunar mass equal to 37 particles or 1.99×10^{24} g per particle. Angular momentum is in units of the current angular momentum of the Earth/Moon system.

method which tracks the evolution of interacting particles using a Lagrangian approach. The SPH method accounts for self-gravity and utilizes similar equations of state as the Kipp and Melosh model. However, the SPH method suffers from its large particle size: one lunar mass is represented by only 37 particles, each with a radius of nearly 500 km.

Table I lists basic results from their runs. Impactors smaller than $\sim 0.14 M_{\oplus}$ (8.4×10^{26} g, or ~415 particles) tend to leave too much iron in bound orbits, while those $\sim 10^{27}$ g in mass (602 particles) are most effective in ejecting large amounts of mantle material. The debris disk is centered roughly at the Roche radius for silicate densities, and iron ejected into orbit from the core of the impactor has a smaller mean orbital radius on average. This basic disk structure is relatively insensitive to the details of the impact event. In some of their simulations, bound clumps of particles remain at the end of the simulation. However, the resolution of the SPH simulations is too poor to obtain detailed information on protolunar disk structure, since in most runs the entire disk is represented by only a few tens of particles (Benz 1994, personal communication).

While extensive modeling efforts have been devoted to the formation of an impact-generated protolunar disk, surprisingly little has been done to explain how such a disk could accumulate into a single, large Moon. From the morphology of the satellite systems of the outer planets, one might naturally expect that a protolunar disk centered around the Roche limit would evolve into a system of multiple moons and rings. Past workers have suggested that multiple moonlets which accreted in the protolunar disk evolved into crossing orbits due to tidal orbital evolution, allowing for their subsequent accumulation to form a single Moon (Ruskol 1973, 1977, Cameron 1986). However, the eventual crossing of moonlet orbits requires that the *innermost* moonlet which forms in the disk be the most massive (Cameron 1986, Cameron and Benz 1991). This is contrary to the character of all other satellite systems and to the pattern of accretional growth in the Roche zone presented in Canup and Esposito (1995, hereafter CE95).

In an unpublished work, (D. Spaute and W. K. Hartmann, personal communication, 1988; Hartmann, personal communication, 1994) modeled accretion in multiple zones of a circumterrestrial disk using an early version of the Spaute *et al.* (1991) planetary accretion code. They found that in a centrally condensed disk, accretional growth proceeds most rapidly at the inner edge of the disk due to enhanced collision frequencies. They proposed that accretion in a centrally condensed disk could lead to moonlets which decrease in mass with orbital radius. This would allow for bodies in the inner disk to evolve outward at a relatively faster rate and sweep-up exterior material to yield a single Moon. Spaute and Hartmann used a two-body criterion for accretion which did not account for three-body tidal effects. However, our recent work has shown that tidal forces affect accretional growth in an entire region surrounding the Roche radius, which we call the Roche zone (CE95).

In this paper we apply the accretion model developed in CE95 to accretion in an impact-generated protolunar disk, adding consideration of orbital evolution due to tidal interaction with the Earth. The character and evolution of an impact-generated disk in its earliest stages, in which a disk likely composed of gaseous and/or liquid/molten components viscously spread and cooled (and possibly became gravitationally unstable; Thompson and Stevenson 1988), have not been well modeled. We concentrate this study on the next phase of disk evolution—when disk

material has cooled and settled enough to allow for the accretional growth of moonlets. We use our accretion and orbital evolution models to constrain the physical parameters of a disk which could lead from the onset of this second phase to the eventual accretion of a single lunar-sized body. We also examine how processes occurring prior to collisional growth, such as instability or early condensation of high density materials, might help to "seed" growth of a single Moon. Throughout this work, we consider limiting conditions (e.g., completely inelastic collisions with no fragmentation or erosion) which all favor accretional growth. Even with these assumptions, we identify only a few scenarios in which a single Moon results (Table II). It is our hope that this work will encourage additional higher-resolution simulations of the impact event and modeling of the earliest stages of disk evolution, to determine which, if any, of the formation scenarios are most physically plausible.

In Section II we discuss physical processes important in an impact-generated disk, including collisions and orbital evolution. In Section III we derive scaling expressions for collisional zone widths and moonlet masses valid for accretion in the Roche zone. Criteria for moonlets to evolve into crossing orbits are derived in Section IV, and used in conjunction with our tidal accretion model in Section V to constrain the radial surface density profile of a protolunar disk required to yield a single Moon. Comparisons with impact simulation results are then made in Section VI. In Section VII, we outline formation scenarios involving processes in addition to the collisional growth of lunar density material which could also lead to the accumulation of the protolunar disk into a single body. Our conclusions are presented in Section VIII.

II. DISK PROCESSES

While numerical simulations cannot predict detailed initial disk conditions, they do show features which seem relatively insensitive to the specifics of an impact, including the creation of a dense, centrally condensed disk and temperatures of at least 1500–2000 K. Collisions between gas-molecules or orbiting bodies will damp relative energies, causing the disk to flatten, and transport angular momentum, causing the disk to spread. Viscous spreading in the early disk may have been extremely rapid, especially if, for example, gas in the disk were turbulently convective. Cooling will occur prior to condensation and/or solidification, whether ejected material is initially vaporized or molten. Collisions between solid objects will result in fragmentation for high impact velocities. When relative velocities between orbiting objects have sufficiently damped, accretional growth may begin. As massive bodies accrete in the disk they will experience orbital evolution due to tidal interaction with the Earth.

Although this general scenario involves a wide array of physical processes, we can identify the most important by consideration of their relative rates. By far the fastest process is collisional evolution, with each particle experiencing a collision in time $t_{\rm col}$,

$$t_{\rm col} \sim \frac{1}{\tau\Omega} \sim 28 \left(\frac{r}{1\ \rm km}\right)\left(\frac{a}{3R_\oplus}\right)^{3/2}\left(\frac{\sigma}{1\times 10^6 \rm g/cm^2}\right)^{-1} \quad \rm min, \tag{1}$$

where τ is optical depth, Ω is orbital frequency, r is particle radius, a is orbital radius, $R_\oplus$ is the radius of the Earth, and σ is the disk surface density. Typical values for σ range from 10^7g/cm^2 at $2R_\oplus$ to 10^5g/cm^2 at $4R_\oplus$ (Cameron 1994). Disk flattening due to collisional dissipation will occur on timescales of many orbits (depending on the degree of collisional elasticity), implying a timescale of days to weeks. Cooling timescales for a gaseous disk radiating as a blackbody are on the order of

$$t_{\rm cool} \sim \frac{M_{\rm d} C T}{2\pi r_{\rm d}^2 \sigma_{\rm SB} T^4} \sim 6 \left(\frac{r_{\rm d}}{3R_\oplus}\right)^{-2}\left(\frac{T}{2000\ \rm K}\right)^{-3}\left(\frac{M_{\rm d}}{2M_{\rm M}}\right) \rm years \tag{2}$$

(Thompson and Stevenson 1988) and may be significantly longer due to latent heat of phase changes (Stevenson 1987). Here $M_{\rm d}$ and $r_{\rm d}$ are the total mass and radial width of the protolunar disk, $M_{\rm M}$ is a lunar mass, C is specific heat, T is temperature in kelvins, and $\sigma_{\rm SB}$ is the Stephan–Boltzman constant. In general, a gaseous disk will have spreading timescales due to angular momentum transport much longer than its characteristic cooling time. This led Cameron and Ward (1976) to propose that a protolunar disk would cool rapidly to form a massive analogue of the rings of Saturn. However, Thompson and Stevenson (1988) predict timescales for viscous spreading in a two-phase vapor/liquid protolunar disk of only 100 years. Thus spreading of disk material prior to disk cooling and accretional growth is expected, depending on the exact physical state of ejected material.

Collisions

An initially spheroidal cloud or fat disk produced by a giant impact will rapidly flatten due to interparticle collisions. The initial size distribution of particles in the disk depends on the nature of the ejected material. A vapor or vapor/fluid disk would likely condense into droplet size particles, while if debris is ejected in large magma clumps, initial particle sizes may be much larger. In either case, the effects of collisions will dominate disk evolution once the disk has cooled enough to allow for solidification. Experimental results have shown that solid rocks frag-

ment at collision velocities greater than 50–100 m/sec (e.g., Hartmann 1978). Relative disk velocities would be at least this high until eccentricities were damped $\lesssim$0.01–0.02 at $3R_\oplus$ and the disk scale height was on the order of $0.05R_\oplus$. When collisions have further dampled relative velocities in the disk to $\sim v_{esc}$ of the largest bodies (approximately centimeters-per-second to meters-per-second for meter- to kilometer-sized bodies), accretional growth may begin (see Section III for a detailed description).

Orbital Evolution

Objects in the protolunar disk experienced orbital evolution as they interacted with tidal bulges raised on the Earth. The rate of evolution of the semi-major axis of a body in Earth orbit due to tides raised on the Earth is approximately given by

$$\frac{da}{dt} \approx 3k_2 \sqrt{\frac{G}{M_\oplus}} R_\oplus^5 m a^{-11/2} \sin(2\delta_s) \tag{3}$$

where k_2 is the Earth's tidal Love number, $M_\oplus$ and $R_\oplus$ are the mass and radius of the Earth, m and a are the mass and orbital radius of the orbiting body, and δ_s is the lag angle between the bulge raised on the Earth and point below the disturbing body (e.g., Burns 1986). For orbiting bodies outside synchronous orbit, da/dt is positive. The tidal Love number is related to the internal structure of the perturbed material and its self-gravity; k_2 for the present day Earth is $\sim$0.25 (e.g., Burns 1986). The quantity $\sin(2\delta_s)$ is usually approximated by $1/Q$, where Q is the specific tidal dissipation function of the Earth. Large amounts of dissipation lead to large lag angles, small values of Q, and rapid evolution rates. The current value of Q for the Earth is $Q \sim 12$, an extremely low value likely due to efficient dissipation in oceans (see Burns 1986).

Integrating Eq. (3) (assuming a constant value of Q) yields orbital radius as a function of time

$$a(t) = \left(\frac{13}{2} Kmt + a_0^{13/2}\right)^{2/13} \tag{4}$$

or the time to reach radius a_1 from a_0

$$t = \frac{a_1^{13/2} - a_0^{13/2}}{Km}, \tag{5}$$

where

$$K \equiv \frac{1}{Q} 3k_2 \sqrt{\frac{G}{M_\oplus}} R_\oplus^5. \tag{6}$$

The expressions given in Eqs. (3)–(5) are poor approximations for orbits near synchronous orbit, since for $a = a_{sync}$, $\delta_s = 0$ and no tidal evolution occurs. For orbits near a_{sync}, δ_s is also a function of $(\omega - n)$, where ω is the planet's angular velocity, n is the mean motion of the disturbing body, and da/dt is zero for $a = a_{sync}$ (Burns 1973). The location of Earth's synchronous orbit was interior to its current position at the onset of lunar formation. The total angular momentum of the current Earth/Moon system implies a rotation period of 4.1 hr for a single body; simulations of impact events produce Earth rotation period of 5 hr or less (Benz *et al.* 1989). Thus a_{sync} after the impact even was likely $\sim$2–$2.5R_\oplus$; all material exterior to this would have evolved outward due to tidal interaction with the Earth.

Orbital evolution will occur on longer timescales than accretional growth within a collisional zone in the protolunar disk. The radial spacing between bodies which have accreted in neighboring zones in a disk is typically estimated to be the maximum range over which the bodies can gravitationally perturb one other into crossing orbits (e.g., Birn 1973, Wetherill and Stewart 1993, Lissauer 1995). This range is approximately

$$\Delta a \approx 3.5 R_{Hill} \tag{7}$$

(e.g., Petit and Henon 1986, Gladman 1993), where R_{Hill} is the mutual Hill radius of the interacting bodies:

$$R_{Hill} = a \left(\frac{m_1 + m_2}{3M_\oplus}\right)^{1/3}. \tag{8}$$

Equation (7) represents the maximum distance over which an object on a circular orbit can perturb the orbit of another body during a single encounter and has been verified by numerical three-body simulations (e.g., Petit and Henon 1986). Additionally, Gladman (1993) has numerically confirmed Δa for long times and repeat encounters. The actual spacing between bodies which initially accrete in a disk may be somewhat larger than that indicated in Eq. (7), as a ''chaotic zone'' of interaction extends beyond the Hill stability limit (Gladman 1993). However, for bodies of $0.1M_\oplus$ or larger in Earth orbit this increases the spacing between neighboring moonlets by less than 15% (see Gladman 1993, his Fig. 8a). Here we will consider the radial separation between moonlets in neighboring zones to be the standard relation in Eq. (7).

The time it takes a body of mass m to tidally evolve a distance of 3.5 times its Hill radius, i.e., the time it takes a body to orbitally evolve through the radial width of its initial feeding zone, can be found from Eqs. (5) and (7):

$$t_{evol} \sim 25 \left(\frac{a_0}{3R_\oplus}\right)^{13/2} \left(\frac{m}{M_\oplus}\right)^{-2/3} \text{years}, \tag{9}$$

assuming $(m/3M_\oplus)^{1/3} \ll 1$ and $Q = 12$. Since the Q value

for Earth in the past was likely larger than its current value even for a partially molten Earth (Ross and Schubert 1989), and the rate expression in Eq. (3) overestimates orbital evolution rates near synchronous orbit, Eq. (9) likely underestimates the time required for an object to evolve out of its feeding zone. Nevertheless, t_{evol} is much longer than collisional (approximately minutes to hours) and orbital (4–15 hr for $a \sim 2$–$5R_\oplus$) timescales even for large bodies, and accretion of moonlets within each collisional zone will occur prior to orbital evolution of bodies into exterior zones.

III. ACCRETION OF MOONLETS

For orbits exterior to the Roche zone, all material contained in a collisional zone will accumulate into a single body whose mass is given by

$$m_L = 2\pi a \Delta a \sigma, \tag{10}$$

where m_L is the mass of the moonlet, Δa is the radial spacing between moonlets in neighboring zones given in Eq. (7), and σ is the surface mass density of the disk at radius a. Equations (7) and (10) can be combined to yield expressions for Δa and m_L exterior to the Roche zone in terms of disk surface density;

$$m_L \approx 62 a^3 \sqrt{\frac{\sigma^3}{M_\oplus}} \tag{11}$$

and

$$\Delta a \approx 10 a^2 \sqrt{\frac{\sigma}{M_\oplus}} \tag{12}$$

(e.g., Lissauer 1995).

Within the Roche zone accretional growth is limited by tidal forces. In CE95, we developed an analytical model and a numerical simulation of accretion which account for the tidal effects of the central planet. We derived "three-body" accretion criteria based on the requirement that two bodies must have a total energy less than that of the closed potential surface of their mutual Hill sphere in order for them to remain gravitationally bound. This requirement yields two accretion criteria. First, the coefficient of restitution, ε, must be less than a critical value, $\varepsilon_{crit,3B}$, for accretion to occur. Second, the sum of the radii of the colliding bodies must be smaller than the angle-averaged width of their mutual Hill sphere in order for the pair to remain bound, even for completely inelastic collisions.

The first accretion criterion is

$$\varepsilon < \varepsilon_{crit,3B} \equiv \sqrt{\left(\left(\frac{v_e}{R_{Hill}\Omega}\right)^2 + \frac{2}{3}r_p^2 - 9\right) \Big/ \left(\left(\frac{v_e}{R_{Hill}\Omega}\right)^2 + \left(\frac{v_{rel}}{R_{Hill}\Omega}\right)^2 + \frac{2}{3}r_p^2\right)}, \tag{13}$$

where v_e is the two-body mutual escape velocity ($v_e = \sqrt{2G(m_1 + m_2)/(r_1 + r_2)}$), v_{rel} is the relative velocity neglecting mutual gravity between the orbiting bodies

$$v_{rel}^2 = (a\Omega)^2(e^2 + i^2) - \tfrac{3}{4}b^2, \tag{14}$$

(where e and i are eccentricity and inclination and $b = (a_1 - a_2)$ is the separation in semi-major axis), and r_p is the ratio of the sum of the radii of the colliding particles to their mutual Hill radius (see CE95 for a complete description). In a tidal potential, impact velocity is a function of the orientation of the impact, and Eq. (13) was derived by averaging uniformly over all possible impact orientations. In reality, low-velocity collisions between bodies on nearby orbits would likely exhibit preferred, non-random collisional alignments. *In order to remove the dependence of our results on impact orientation, we consider only* $\varepsilon = 0.0$ *collisions,* so that the assumption of complete inelasticity removes any dependence of accretion on impact velocity.

Even if two bodies collide inelastically, they will not remain bound if their energy is greater than the closed potential surface of their Hill sphere. This is the case if the bodies physically overflow their Hill sphere. The sum of the radii of the colliding bodies scaled by their mutual Hill radius, r_p, can be expressed as

$$r_p = \frac{r_1 + r_2}{R_{Hill}} \approx 0.6 \left(\frac{a}{a_{Roche}}\right) \frac{1 + \mu^{1/3}}{(1 + \mu)^{1/3}}, \tag{15}$$

where a_{Roche} is the Roche radius

$$\frac{a_{Roche}}{R_\oplus} = 2.456 \left(\frac{\rho}{\rho_\oplus}\right)^{-1/3}, \tag{16}$$

r_1, r_2, and ρ are the radii and density of the colliding bodies, $\rho_\oplus$ is the density of the Earth, and μ is the mass ratio of the colliding bodies with $0 < \mu \leq 1$. Equation (15) demonstrates that near the Roche limit, $r_p \sim R_{Hill}$. The Hill sphere is actually an asymmetric lemon-shaped surface, whose half-widths in the radial, azimuthal, and vertical dimensions are respectively $1R_{Hill}$, $\frac{2}{3}R_{Hill}$, and $\sim 0.64R_{Hill}$. It is reasonable to assume that a pair of objects would rotate through a variety of orientations following a collision, as the collision would almost certainly yield a pair with some angular momentum. Weidenschilling *et al.* (1984)

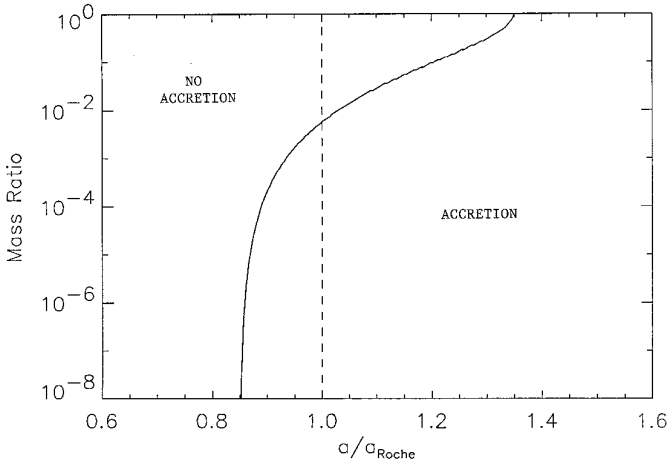

FIG. 1. The critical mass ratio curve for accretion as a function of $a/a_{\rm Roche}$. A mass ratio of unity corresponds to collisions between like-sized objects. To the left of the curve, accretion is precluded by tidal forces *even for completely inelastic collisions.* To the right of the curve, accretion is possible depending on impact velocity, impact and rebound orientation, and the coefficient of restitution.

estimated spin rates for like-sized bodies undergoing inelastic collisions to be on the order of the orbital frequency. With this in mind, we require that the colliding bodies must not physically overflow the angle-averaged width of their mutual Hill sphere in order for them to remain gravitationally bound subsequent to a completely inelastic collision. This yields an $r_{\rm p} \lesssim 0.7$ condition. If we assumed that a pair rotated through all orientations, a more appropriate choice would be an $r_{\rm p} \lesssim 0.64$ criterion, requiring that the pair not overflow the narrowest dimension of their Hill sphere in order to remain bound. Three-body simulations by Ohtsuki (1993), which include collision-induced rotation, show a rapid decrease in accretion probability for $\varepsilon = 0.0$ collisions from $r_{\rm p} = 0.6$ (with a capture probability of about 85%) to $r_{\rm p} = 0.7$ (with a capture probability of less than 10%, see his Fig. 8). We will use an $r_{\rm p} \lesssim 0.7$ criterion in this work, and assume all collisions which satisfy this condition result in accretion.

For a given orbital radius and particle density this criterion defines a critical mass ratio for accretion:

$$\frac{(1+\mu_{\rm crit})^{1/3}}{1+\mu_{\rm crit}^{1/3}} \approx 2.1 \frac{R_\oplus}{a}\left(\frac{\rho}{\rho_\oplus}\right)^{-1/3}. \qquad (17)$$

Here $\mu_{\rm crit}$ is the maximum mass ratio that two bodies can have in order to satisfy the $r_{\rm p} \lesssim 0.7$ condition following a completely inelastic collision. The critical mass ratio accretion curve as a function of $(a/a_{\rm Roche})$ is shown in Fig. 1. Altering the critical $r_{\rm p}$ value shifts to curve slightly to the left or right (for higher or lower critical $r_{\rm p}$ values, respectively) but does not affect its shape. Inside the Roche radius, accretion is possible only between bodies which differ greatly in size (i.e., with small mass ratios), while accretion is precluded between like-sized bodies well outside the Roche limit even for completely inelastic collisions. The transitional regime surrounding the Roche radius where tidal forces modify the character of accretional growth will be referred to as the "Roche zone."

Figure 2 contrasts the accretional evolution of a silicate distribution within and exterior to the Roche zone at orbital radii of 3 and $4R_\oplus$ assuming $\varepsilon = 0.0$, using the numerical simulation described in CE95. In this model, the mass and velocity evolution of an accreting swarm are followed with a Markov formalism, whose results represent expectation values for the swarm population as a function of time (see CE95 for details). This simulation considers the same basic accretion physics as the Greenberg *et al.* (1978) and Spaute *et al.* (1991) models of planet formation, except that we implement the three-body accretion criteria described above in order to account for tidal effects important in the Roche zone. We utilize the work of Stewart and Wetherill (1988) to model velocity evolution due to rebounding collisions and distant encounters, and also consider velocity evolution due to accretion in an analogous approach (CE95, Appendix B). Figure 2 shows that outside the Roche zone, the swarm rapidly re-accretes into a single body, while within the Roche zone the end result is a distribution of moonlets.

In the extreme case of completely inelastic collisions, accretion in the Roche zone thus proceeds until all of the mass within a collisional zone is contained in a distribution of bodies too close in mass to accrete. The maximum extent of accretion in the Roche zone yields a distribution of moonlets, which can be described by a power-law:

$$n(m)dm = Cm^{-q_m}dm \qquad (18)$$

$$\mu_{\rm crit} m_{\rm L} \le m \le m_{\rm u}. \qquad (19)$$

Here $n(m)dm$ is the number of bodies with mass in the range $[m, (m + dm)]$, q_m is the differential mass exponent of the moonlet distribution, $\mu_{\rm crit}$ is the critical mass ratio for accretion defined in Eq. (17), and $m_{\rm u}$ is the upper limit of the differential mass distribution, defined as in Lissauer and Safronov (1991) to be

$$m_L \approx \int_{m_{\rm L}}^{m_{\rm u}} n(m')m'dm', \qquad (20)$$

where $m_{\rm L}$ is the mass of the largest body in the distribution.

Relations analogous to Eqs. (11) and (12) can be derived for accretion within the Roche zone. Let M be the total amount of mass in a collisional zone so that

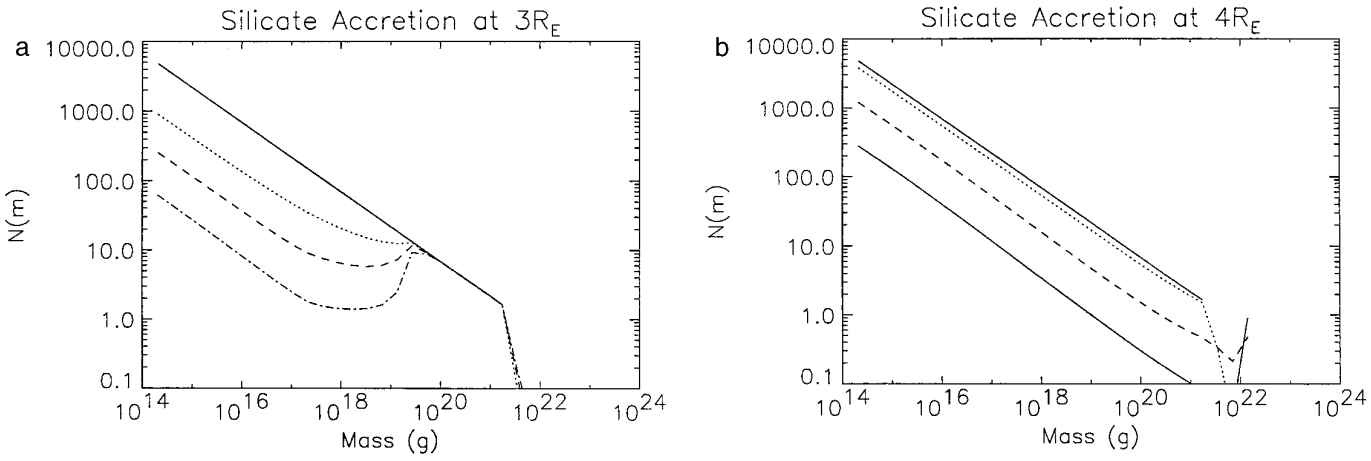

FIG. 2. (a) The accretional evolution of a distribution of silicates at $a = 3R_\oplus$, assuming completely inelastic collisions. The initial distribution has an optical depth of $\sim 5 \times 10^{-3}$. Solid, dotted, dashed, and dot-dashed lines correspond to mass distributions at $t = 0$, 2.5, 4.6, and 7 months. Here tidal forces limit accretional growth of the largest bodies. (b) The evolution of the same initial distribution as in (a), but here $a = 4R_\oplus$, just exterior to the Roche zone. Here, solid, dotted, dashed, and dot-dashed lines correspond to mass distributions at $t = 0$, 0.8, 8, and 44 months. After 3.7 years, there is a 95% probability that all material has accumulated into a single body of mass 1.4×10^{22} g.

$$M = 2\pi a \Delta a \sigma, \tag{21}$$

where Δa is the width of the zone. The largest value for m_L for a distribution of moonlets is obtained by setting the number of bodies of mass m_L equal to 1, or

$$N(>m_L) \equiv 1 = \frac{C}{q_m - 1} m_L^{-(q_m - 1)}, \tag{22}$$

where the constant in the cumulative mass distribution is $(C/(q_m - 1))$ and the cumulative exponent is $(q_m - 1)$. From Eqs. (20) and (22), the relation between the upper limit to the differential distribution and the mass of the largest body is:

$$\frac{m_u}{m_L} = \left[1 - \left(\frac{q_m - 2}{q_m - 1}\right)\right]^{1/(2 - q_m)}. \tag{23}$$

Setting M equal to the total mass found by integrating $mN(m)$ over the range given by Eq. (19) then gives m_L as a function of M, q_m, and μ_{crit}:

$$m_L = \left(\frac{(q_m - 2)}{(q_m - 1)\left(\mu_{crit}^{2 - q_m} - 1 + \left(\frac{q_m - 2}{q_m - 1}\right)\right)}\right) M. \tag{24}$$

Combining Eqs. (7), (21), and (24) yields

$$m_L = \left(\frac{(q_m - 2)5\pi}{(q_m - 1)(\mu_{crit}^{2 - q_m} - 1 + ((q_m - 2)/(q_m - 1)))}\right)^{3/2} a^3 \sqrt{\frac{\sigma^3}{M_\oplus}}, \tag{25}$$

and

$$\Delta a = 2.5 \left(\frac{(q_m - 2)5\pi}{(q_m - 1)(\mu_{crit}^{2 - q_m} - 1 + ((q_m - 2)/(q_m - 1)))}\right)^{1/2} a^2 \sqrt{\frac{\sigma}{M_\oplus}}, \tag{26}$$

which are equivalent to Eqs. (11) and (12) when $\mu_{crit} = 1$. The Δa width in Eq. (26) is much narrower for orbits in the Roche zone than would be predicted from the standard expression given in Eq. (12). The mass of the largest moonlet which forms in the Roche zone, m_L, is a function of orbital radius, surface density, the slope of the distribution of accreted bodies, and the critical mass ratio for accretion, μ_{crit}.

This analytical derivation of m_L compares well with results from simulations using our numerical accretion model. In the protolunar disk, particle masses at the onset of accretional growth are likely to be much smaller than the total amount of mass contained in their collisional zone, due to both the severity of the giant impact event and extensive fragmentation prior to accretional growth. Figure 3a shows the evolution of such a size distribution of silicate-density material at $3.3R_\oplus$ ($a/a_{Roche} = 1.14$), with

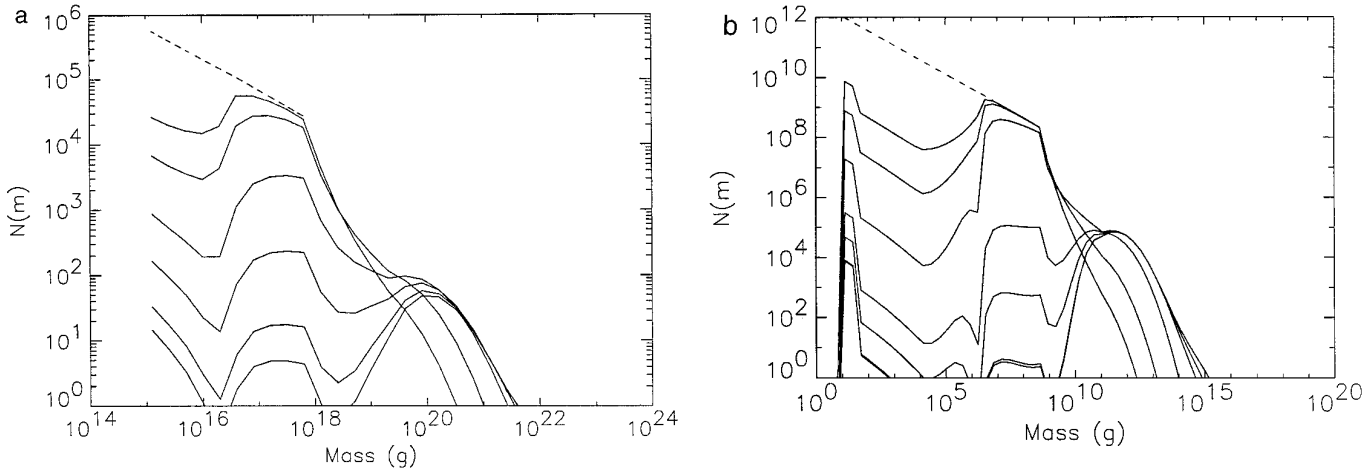

FIG. 3. (a) The evolution of a mass distribution of silicate-density material at $3.3R_\oplus$ ($a/a_{\rm Roche} = 1.14$). The dashed initial distribution has $q_m = 1.5$, a surface density of 10^6 g/cm^2, and $v_{\rm ran} = 5$ m/sec. The total mass in the swarm is 8×10^{22} g, and collisions are assumed to be completely inelastic. Distributions are shown at times $t = 0$, 1, 2, 3, 5, 7, and 8 hr. At $t = 8$ hr, the distribution of the largest bodies (mass $> 5 \times 10^{20}$ g) has a differential mass slope of $q_m \sim 2.7$. Equation (24) predicts the mass of the largest moonlet which accretes for this case should be $\sim 5 \times 10^{21}$ g. (b) The evolution of a mass distribution of silicate-density material at $2.8R_\oplus$ ($a/a_{\rm Roche} = 0.97$). The dashed initial distribution has $q_m = 1.5$ and the total swarm mass is 5×10^{17} g. Distributions are shown at times $t = 0$, 1, 1.4, 2.4, 6, 9, and 12 days; accretion times are longer here than in (a) due to a much lower initial optical depth. The final distribution of large bodies (mass $> 10^{12}$ g) has a differential mass slope of $q_m \sim 2.6$. Equation (24) predicts the mass of the largest moonlet which accretes for this case should be $\sim 6 \times 10^{15}$ g.

an initial surface density of $\sigma = 10^6$ g/cm^2, a critical mass ratio for accretion of approximately $\mu_{\rm crit} \sim 0.06$, and a total feeding zone mass of $M = 8 \times 10^{22}$ g. The initial distribution has a nominal differential mass exponent of $q_m = 1.5$, and a mean time between collisions of $\sim$2 min. In order to consider the most favorable case for accretion, all collisions are assumed to be completely inelastic ($\varepsilon = 0.0$). The distribution of the largest bodies in the $\sim 2 \times 10^{20}$–5×10^{21} g mass range has a steep slope with $q_m \sim 2.7$. In the final distribution, 90% of the mass in the system is contained in moonlets with masses in this range. Eq. (24) predicts $m_{\rm L} \approx 5 \times 10^{21}$ g. The ''waves'' which appear in the distributions (and in those in Figs. 3b and 15) are a result of the fact that bins within a certain range in mass (determined by $\mu_{\rm crit}$) cannot accrete with one another due to tidal constraints. In this case, bodies in the five initially largest mass bins cannot mutually accrete. After 1 hr, small bodies have accreted onto bodies in the largest five bins, causing the first ''wave'' as the small end population is depleted. This is analogous to the pattern seen in Fig. 2a. Here there is enough mass in small particles to slowly populate the unoccupied bins ($>10^{18}$ g) through collisions with the initially largest five bins. Bodies in the largest initial bin (which contain most of the mass in the system) can accrete only onto bodies of mass $\geq 2 \times 10^{20}$ g. Once many bodies of this size are formed (after about 2–3 hr) most of the mass in the system is accreted onto them, forming the peak of the second ''wave'' at approximately 2×10^{20} g. The process ends when all bodies occupy bins too close in mass to accrete.

Figure 3b shows the evolution of a silicate distribution at $2.8R_\oplus$ ($a/a_{\rm Roche} = 0.97$) with $\mu_{\rm crit} \sim 0.003$ and a total mass of $M = 5 \times 10^{17}$ g. The accretion times are longer here than in Fig. 3a because a lower initial optical depth (which corresponded to an initial mean time between collisions of $\sim$48 min) was used to allow for consideration of a much broader mass range. In this case, Eq. (24) predicts $m_{\rm L} \approx 6 \times 10^{15}$ g. The final distribution of the largest bodies here has $q_m \sim 2.6$. It is natural to expect that accretion within the Roche zone will yield distributions of accreted bodies with $q_m > 2$. Differential mass exponents less than 2 imply that most of the mass is contained in the largest body, consistent with runaway growth which is precluded by tidal forces within the Roche zone.

IV. EVOLUTION OF MOONLETS INTO CROSSING ORBITS

Accretion within each collisional zone in the protolunar disk will thus progress until all mass in the zone is contained in bodies in the mass range $\mu_{\rm crit} m_{\rm L} < m < m_{\rm L}$. Additional growth can occur as moonlets evolve into colliding orbits with bodies outside of their initial feeding zone due to tidal interaction with the Earth. The dependence of the rate of tidal evolution (Eq. (3)) on m and a thus has important consequences for accretion of multiple moonlets formed in the disk into a single Moon. If the mass of moonlets in the protolunar disk decreases with orbital radius, then the innermost, largest moonlet will orbitally evolve outward at the relatively fastest rate, conceivably accumulating all

exterior material to produce a single Moon. Conversely, if the mass of accreted bodies in the disk increases with orbital radius, bodies in the inner disk will never catch up with exterior bodies and multiple moons will likely result. To first order, the necessary condition for incorporation of the maximum amount of protolunar disk material into a single moon is thus for the bodies which form just outside synchronous orbit to be the most massive bodies in the disk (Cameron 1986, Cameron and Benz 1991). This can be analytically demonstrated as follows.

From Eq. (4), the orbital separation at time t between two moonlets, δa, is just

$$\delta a = (\tfrac{13}{2}Km_2t + a_{2,0}^{13/2})^{2/13} - (\tfrac{13}{2}Km_1t + a_{1,0}^{13/2})^{2/13}, \quad (27)$$

where $a_{2,0} > a_{1,0}$. The time for the orbital separation to equal zero is

$$t(\delta a = 0) = (a_{2,0}^{13/2} - a_{1,0}^{13/2})/\tfrac{13}{2}K(m_1 - m_2). \quad (28)$$

If the inner moonlet is more massive than the outer moonlet ($m_1 > m_2$), the moonlet orbits will cross in a finite time, while if $m_1 < m_2$ the orbits will never theoretically achieve the same orbital radius.

The simple analysis given above neglects orbital crossing which can occur due to mutual perturbations for finite values of δa if

$$\frac{\delta a}{a} \lesssim 3.5\left(\frac{m_1 + m_2}{3M_{\rm E}}\right)^{1/3}. \quad (29)$$

From Eq. (27), the function $\delta a/a$ is just

$$\frac{\delta a}{a} = ((\tfrac{13}{2}Km_2t + a_{2,0}^{13/2})/(\tfrac{13}{2}Km_1t + a_{1,0}^{13/2}))^{2/13} - 1 \quad (30)$$

and its time derivative is

$$\frac{d}{dt}\left(\frac{\delta a}{a}\right) = \frac{K(a_1m_2a_2^{-11/2} - a_2m_1a_1^{-11/2})}{a_1^2}. \quad (31)$$

The sign of $d/dt(\delta a/a)$ is time-independent and only a function of initial masses and orbital positions. If we let $X \equiv (m_1/m_2)$, then $d/dt(\delta a/a)$ will be exactly zero for

$$X = \left(\frac{a_{1,0}}{a_{2,0}}\right)^{13/2}. \quad (32)$$

For X greater than (less than) this ratio, $d/dt(\delta a/a)$ is always positive (negative) and the dynamical separation $\delta a/a$ increases (decreases) with time. In either case, the

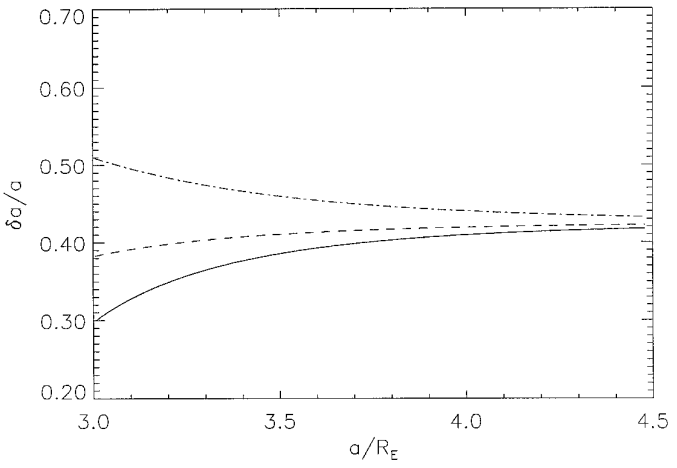

FIG. 4. The scaled orbital separation ($\delta a/a$) between two tidally evolving moonlets with $m_1/m_2 = 0.1$ is shown as a function of orbital radius. The different curves correspond to different initial orbital separations. The solid, dashed, and dot-dashed curves correspond respectively to initial separations of 3.5, 4.5, and $6R_{\rm Hill}$. The asymptotic $\delta a/a$ value is independent of initial orbital positions and is a function only of (m_1/m_2) (see Eq. (34)); here $m_1/m_2 = 0.1$ yields a $\delta a/a = 0.425$ asymptote.

magnitude of $d/dt(\delta a/a)$ decreases with time, since for large t:

$$\frac{d}{dt}\left(\frac{\delta a}{a}\right) \propto \frac{1}{t}. \quad (33)$$

Thus $\delta a/a$ asymptotes to a value of

$$\frac{\delta a}{a} = \left(\frac{m_2}{m_1}\right)^{2/13} - 1 \quad (34)$$

(from Eq. (30)), independent of initial orbital separation. Figure 4 shows the evolution of the dynamical separation $\delta a/a$ between two moonlets with $X = 0.1$ for different initial separations. The solid, dashed, and dot-dashed lines correspond respectively to initial separations of 3.5, 4.5, and $6R_{\rm Hill}$. In each case, the moonlets asymptote to a separation of $\delta a/a = 0.425$ as predicted by Eq. (34). The requirement that this final orbital separation be less than 3.5 Hill radii in order for the moonlets to collide gives:

$$m_2 > \left(\frac{1 - X^{2/13}}{X^{2/13}}\right)^3\left(\frac{1}{3.5}\right)^3\left(\frac{3M_\oplus}{1 + X}\right). \quad (35)$$

Thus for a given value of m_1/m_2, the mass of the exterior moonlet must be larger than that given in Eq. (35) in order for the moonlet orbits to evolve into potentially collisional orbits. This requirement is independent of initial orbital

locations and Q. Figure 5 is a plot of the mass of an exterior moonlet needed for the orbits of two moonlets to evolve into orbits with $\delta a = 3.5R_{\rm Hill}$ as a function of X. A massive exterior moonlet and an inner moonlet which is only slightly less massive than the outer moonlet can tidally evolve into orbits close enough to experience collisions due to mutual perturbations.

Discussion

The implications of Fig. 5 for accretion between bodies with $a_{1,0} < a_{2,0}$ and $m_1 < m_2$ are not obvious. Because two moons with similar masses evolve into orbits close enough to allow for collisions does not necessarily mean that the moons will eventually accrete. Resonances, ''horseshoe'' encounters, or high-velocity collisions could all preclude accretion. When $m_1 \geq m_2$, moonlet orbits will converge until $\delta a = 0$ and so if resonant configurations occurred or velocities were initially too high to allow for accumulation, orbital separation between the bodies would continue to decrease and accretion could become more and more likely. However even in the $m_1 \geq m_2$ case it is important to realize that $\delta a = 0$ does not necessitate accretion. Additional work is required to evaluate accretion probabilities of orbitally evolving moonlets as their orbits cross. Consistent with our approach, we assume the most favorable outcome for accretion.

Zones within the Roche zone contain multiple bodies in the range $\mu_{\rm crit} m_{\rm L} \lesssim m \lesssim m_{\rm L}$. Consider the largest body m_1 which forms in a zone at orbital radius a_1 in the Roche zone, interior to a neighboring zone at a_2. If the largest body in the inner zone is significantly less massive than the smallest body in the exterior zone, i.e., if $m_1 < \mu_{\rm crit} m_2$, all material in the zones will orbitally diverge. In the intermediate case of $\mu_{\rm crit} m_2 < m_1 < m_2$, moonlet m_1 will rapidly overtake less massive material in the outer zone 2, but will be unable to accrete this material since for $m_1 < m_2$,

$$\frac{\mu_{\rm crit} m_2}{m_1} > \mu_{\rm crit} \tag{36}$$

and accretion is tidally precluded. For $m_1 > m_2$, m_1 will overtake all material in the outer zone. In this case, moonlet m_1 can accrete the smaller bodies in zone 2, since here $\mu_{\rm crit} m_2/m_1$ is less than the critical mass ratio for accretion. If $m_1 > m_2$, the inner moonlet m_1 will likely accrete all exterior material. Note that accretion within zones will be completed prior to evolution of bodies into neighboring zones since $t_{\rm col} \ll t_{\rm evol}$ (see Section II).

Although collisions between an interior body and a slightly larger exterior body are possible in the course of tidal orbital evolution, accretion between moonlets with $m_1 \geq m_2$ is much more probable. To first order, the simple requirement that the innermost body which contributes to the Moon must be the most massive is well founded.

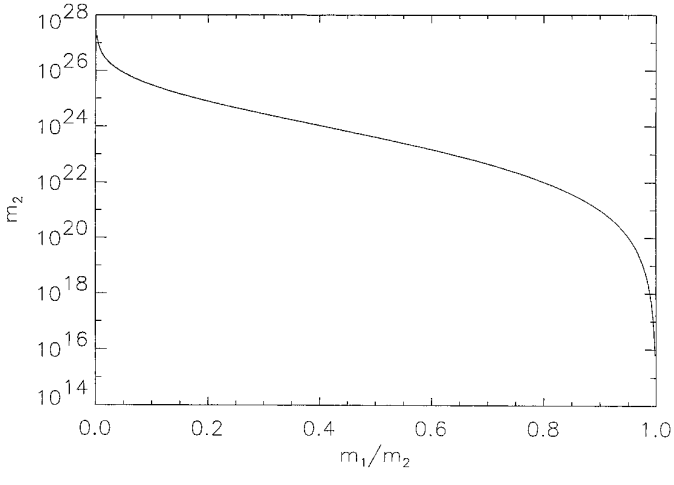

FIG. 5. For two moonlets of mass m_1 and m_2, where m_1 is initially interior to m_2 and $m_1 < m_2$, the outer moonlet (m_2) must have a mass above the curve shown here in order for the two moonlets to tidally evolve into orbits with a separation of less than $3.5R_{\rm Hill}$ (see Eq. (35)). This is the maximum separation over which mutual perturbations can lead to collisions. Thus for a given mass ratio m_1/m_2, there is a minimum mass for m_2 which is necessary for the moonlets to evolve into potentially collisional orbits. If $m_1 > m_2$, the moonlets will tidally evolve into orbits with no orbital separation ($\delta a = 0$) for any value of m_2.

V. SURFACE DENSITY CONSTRAINTS ON THE PROTOLUNAR DISK

The requirement that the mass of the largest body which accretes in a zone decreases with orbital radius can be used to constrain the radial surface density of the protolunar disk needed to yield a single Moon. To first order, the orbital radius at which $dm_{\rm L}/da$ becomes negative is indicative of the innermost region in the disk which would contribute material to form the moon. From Eq. (25), setting $dm_{\rm L}/da = 0$ gives

$$\sqrt{\frac{1}{M_\oplus}\left[\left(\frac{q_m - 2}{q_m - 1}\right) 5\pi\sigma_0 a_0^b\right]^3} \qquad \frac{d}{da}\left(\frac{a^{3-3b/2}}{(\mu^{2-q_m} - 1 + ((q_m - 2)/(q_m - 1)))^{3/2}}\right) = 0, \tag{37}$$

or

$$\frac{-3(2 - q_m)}{2(\mu_{\rm crit}^{2-q_m} - 1 + ((q_m - 2)/(q_m - 1)))}\,\mu_{\rm crit}^{1-q_m} \qquad a\frac{d\mu_{\rm crit}}{da} + \left(3 - \frac{3}{2}b\right) = 0. \tag{38}$$

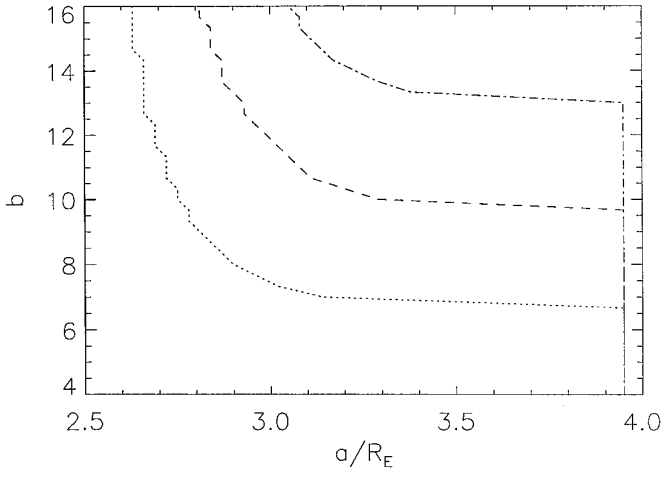

FIG. 6. The orbital radius at which $dm_L/da = 0$ as a function of b, the slope of the radial surface density in the protolunar disk. The classical Roche limit is at $\sim 2.9R_\oplus$. The dotted, dashed, and dot-dashed lines correspond respectively to $q_m = 2.2$, 2.5, and 2.8, where q_m is the differential mass exponent of the distribution of moonlets which accretes in a feeding zone. Numerical simulations of accretion in the Roche zone yield q_m values between 2.5 and 2.8.

Here the radial profile of the disk surface density is modeled as a power-law

$$\sigma(a) = \sigma_0 \left(\frac{a_0}{a}\right)^b, \tag{39}$$

with a_0 the inner radius of the disk and σ_0 the surface density at a_0.

For orbits outside the Roche zone, $d\mu_{crit}/da = 0$ and dm_L/da is negative for $b \geq 2$. Inside the Roche zone, the orbital radius at which dm_L/da becomes negative can be determined numerically as a function of both b (the slope of the radial surface density) and q_m (the slope of the distribution of accreted moonlets within a feeding zone). Figure 6 shows that for small values of b, m_L increases with orbital radius within the Roche zone (i.e., $dm_L/da > 0$ for $a < 4R_\oplus$). In order for dm_L/da to become negative within the Roche zone, the slope of the radial surface density profile, b, must be greater than ~ 10 for values of q_m similar to those predicted by numerical simulations of tidal accretion.

Figure 7 shows distributions of moonlets which accrete in protolunar disks as a function of radial surface density profile. The mass of the largest body which accretes at each orbital radius (Eq. (25)) is plotted for power-law surface density profiles, for both 1 times (stars) and 2 times (crosses) a lunar mass disks with $a_0 = 2R_\oplus$. Collisional zone widths have been calculated from Eq. (26), and a nominal value of $q_m = 2.5$ has been used in all cases. Throughout each zone, a critical mass ratio for accretion appropriate for the outer edge of the zone (where accretion is easiest) has been used to determine m_L. The collisional zones are more closely spaced for higher values of b, since lower surface densities at a given orbital radius yield smaller Δa widths.

Figure 7a represents a disk with a $b = 4.0$ surface density profile. For both the 1 and $2M_M$ cases, the moonlets formed exterior to $\sim 3.5R^\oplus$ evolve into orbits with $\delta a_{min} < 3.5R_{Hill}$. Figures 7b and 7c show analogous distributions for $b = 8$ and 10. In the former case, several of the moonlets which accrete at ~ 2.8–$3.3R_\oplus$ satisfy Eq. (35) with one another, but these moonlets will not experience close approaches with outer moonlets unless they grow in mass. In the $b = 10$ case, all moonlets with $a \gtrsim 2.6R_\oplus$ satisfy the Eq. (35) criterion.

Figure 8a shows the orbital evolution paths of the moonlets which satisfy the $\delta a_{min} < 3.5R_{Hill}$ criterion for the $2M_M$, $b = 4$ disk. Similar patterns are observed for all b values below the critical values shown in Fig. 6. The evolution paths shown correspond to the rates appropriate for the original mass of each moonlet—no accretion between moonlets is assumed. While incorporation of material with $a \lesssim 3.5R_\oplus$ into a single Moon is precluded because Eq. (35) is not satisfied for these inner moonlets, a single Moon can result if the moonlet formed at $\sim 3.5R_\oplus$ accretes with the moonlet formed at $4.2R_\oplus$. This is probable, since their orbital separation will asymptote to $\sim 1.4R_{Hill}$. However, the $4.2R_\oplus$ moonlet might overtake and accrete the $6R_\oplus$ moonlet prior to this. The resulting moonlet and the $3.5R_\oplus$ moonlet asymptote to a $\delta a \sim 2.5R_{Hill}$ separation. Thus for the $b = 4$, $2M_M$ disk, a single Moon of mass $\sim 0.5M_M$ composed from material outside the Roche zone is the end result, assuming moonlets with $\delta a \leq 3.5R_{Hill}$ accrete and that material within the Roche zone eventually re-impacts the Earth. It is significant that the order of accretion events can potentially change the final state of the system by altering the masses and mass ratios of the evolving moons. More detailed simulations are needed to determine the most likely sequence of events as moonlets collide due to orbital evolution into $\delta a = 0$ orbits or perturbations by mutual interaction for $\delta a \leq 3.5R_{Hill}$.

An intermediate case is Fig. 8b, which shows the orbital evolution paths of moonlets from the $b = 8$, $2M_M$ disk. Here the three inner moonlets, which have a total mass of 10^{24} g, quickly occupy colliding orbits. Meanwhile, moonlets formed at 3.6, 4.0, and $4.8R_\oplus$ evolve into $\delta a < 3.5R_{Hill}$ orbits in less than 1000 years, presumably accreting to form a body of $\sim 3 \times 10^{24}$ g, or $0.04M_M$. A single moon could result from this disk, but would likely contain much less than a lunar mass of material, since positive values of dm_L/da for $a < 4R_\oplus$ make it difficult for inner bodies to sweep up material they overtake in the Roche zone.

Radial surface density profiles which have power-law exponents greater than or equal to the critical values of b

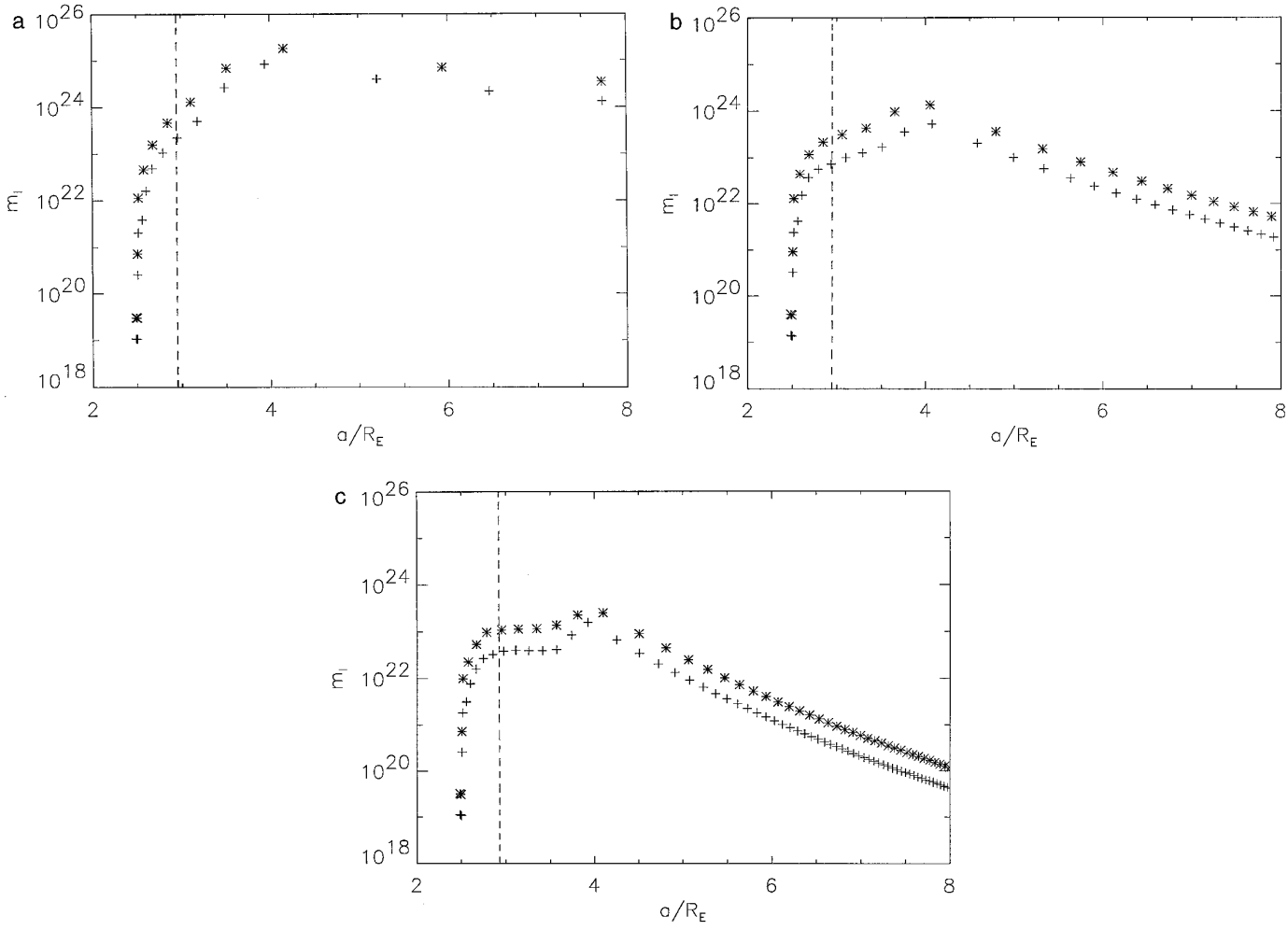

FIG. 7. The distribution of moonlets which accrete in the protolunar disk as a function of orbital radius. Here m_L is the mass of the largest body which accretes in a given collisional zone, and the surface density has been modeled as a power law with $\sigma(a) \propto (1/a)^b$. One and two lunar mass disks are represented by crosses and stars, respectively; the dashed vertical line is the Roche limit for silicates. Figures a–c correspond to b values of 4, 8, and 10, respectively.

in Fig. 6 yield $dm_L/da \leq 0$ within the Roche zone. Figure 9 shows moonlet distributions for 1 M_M disk with $b = 15$. A profile this steep is needed for the largest moonlet which accretes to form within the Roche zone at about $2.8R_\oplus$ (the orbital radius at which the critical b curve for $q_m = 2.5$ asymptotes in Fig. 6).

These results suggest two forms of radial disk distributions which could evolve into a single lunar-sized body. The simplest case is a disk with $b \geq 2$ and at least a lunar mass of material beyond the Roche zone ($a \gtrsim 3.5$–$4R_\oplus$). The second case is a disk with an extremely steep radial density profile ($b \gtrsim 10$), which allows for incorporation of material with initial orbital radii $\gtrsim 2.8R_\oplus$. Intermediate radial surface density profiles do not typically have a lunar mass of material beyond the Roche zone, and yield increasing moonlet mass with orbital radius in the Roche zone.

Discussion

The derivation of the mass of moonlets which accrete in the protolunar disk as a function of orbital radius and surface density presented above has considered the case of completely efficieint accretion of all bodies which satisfy the $\mu < \mu_{crit}$ tidal capture criterion. Competing effects, namely erosion and collisional elasticity, have been neglected. These effects will make the orbital radius at which dm_L/da becomes negative even larger than that shown in Fig. 6 for given values of b and q_m.

Erosion processes will cause the lower limit of the moonlet distribution to be significantly lower than $\mu_{crit} m_L$. Collisions can knock off previously accreted, loosely bound debris and will replenish the low-mass end of the mass distribution in a feeding zone. This will also cause the mass of the largest moonlet which accretes in a zone to be smaller

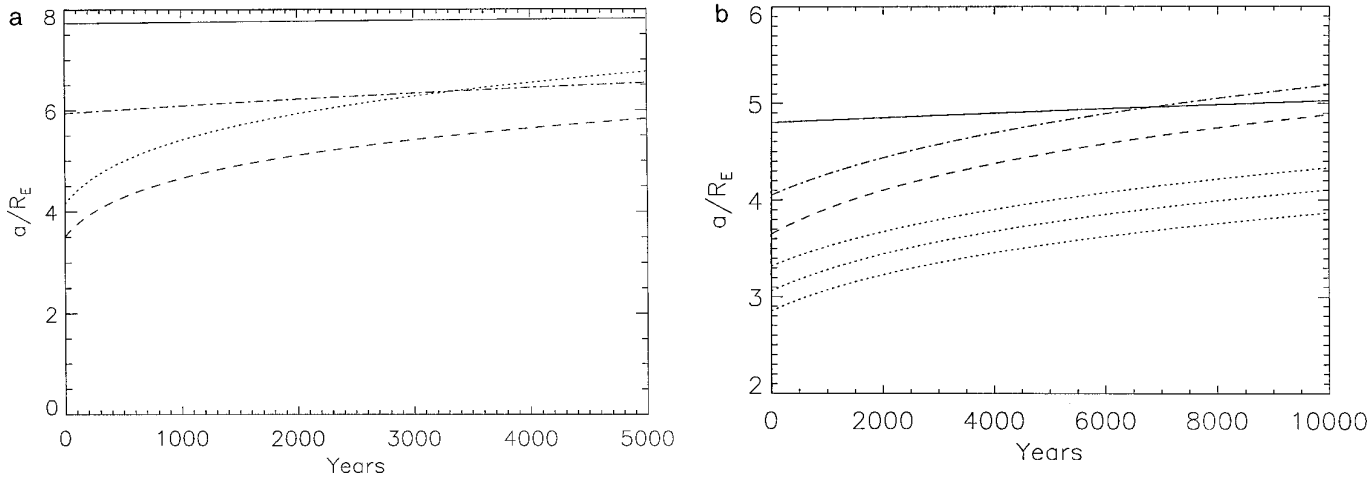

FIG. 8. The orbital evolution paths of moonlets from the two lunar mass, $b = 4$ and $b = 8$ cases in Figs. 7a and 7b. Here each path represents the evolution rate determined by the initial moonlet masses; accretion between moonlets as their orbits cross has not been included.

than in the purely accreting case given in Eq. (25). Minimum collision velocities will be higher in more interior orbits due to greater differences in Keplerian velocity across a body. Erosive effects will cause m_L to be a stronger function of orbital radius than is indicated by Eq. (38).

Collisional elasticity will preclude accretional growth for collisions where the coefficient of restitution, ε, is too large, or when $\varepsilon > \varepsilon_{\text{crit,3B}}$ (Eq. 13). For a given degree of collisional elasticity, accretion in the Roche zone will be increasingly difficult as orbital radii decrease and/or as the mass ratio of colliding bodies increases. Accretion with a non-zero coefficient of restitution requires (from Eq. 13)

$$6/r_p(1 - \varepsilon^2) + \tfrac{2}{3}r_p^2(1 - \varepsilon^2) - 9 \geq 0, \qquad (40)$$

where r_p is the ratio of the sum of the radii of the colliding bodies to their mutual Hill radius, and v_{rel} (the relative velocity between two orbiting bodies neglecting their mutual gravity) has been set equal to zero. Equation (40) defines a new maximum value of r_p for accretion as a function of ε, which in turn defines new critical mass ratios for accretion as a function of ε and orbital radius. Figure 10 shows the critical mass ratio curves for $\varepsilon = 0$, 0.1, 0.25, and 0.5. A given amount of collisional elasticity effectively shifts the Roche zone outward to larger orbital radii. If collisions in the protolunar disk were characterized by $\varepsilon = 0.5$, material within $\sim 3.4R_\oplus$ would not accrete at all, and a very steep radial disk surface density profile would

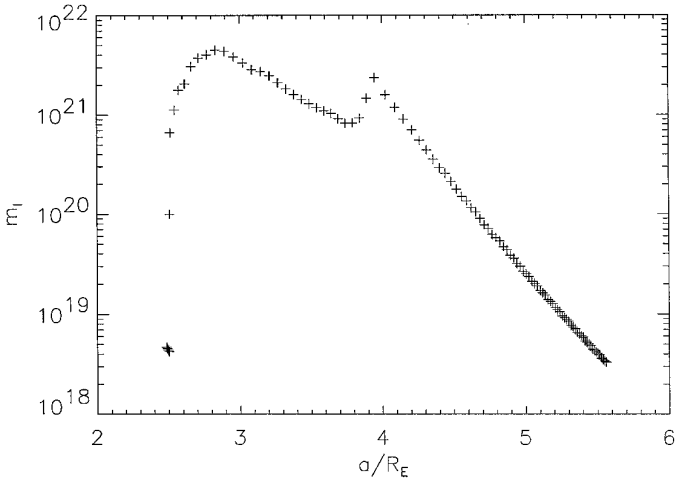

FIG. 9. Moonlets formed in a one lunar mass disk with $b = 15$. The close spacing of bodies in the outer disk is due to the very low surface densities.

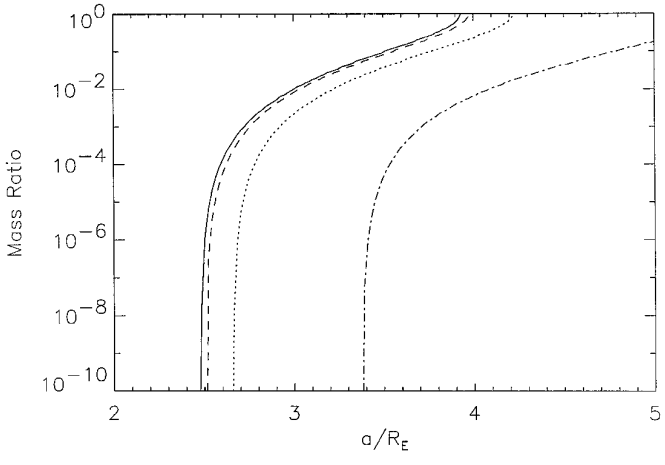

FIG. 10. The critical mass ratio for accretion as a function of orbital radius for silicate density material. The solid line corresponds to completely inelastic $\varepsilon = 0$ collisions, while the dashed, dotted, and dot-dashed lines correspond to $\varepsilon = 0.1$, 0.25, and 0.5, respectively. A non-zero coefficient of restitution effectively shifts the Roche zone outward.

only allow for incorporation of material with $a \gtrsim 3.8R_\oplus$. However, it is possible that collisions between molten rocks in the protolunar disk were very inelastic, and the $\varepsilon = 0$ or 0.1 curves may be more appropriate.

Thus the extreme case of completely inelastic collisions and no collisional erosion considered in this analysis produces the least restrictive conditions for incorporation of material in low orbits into a single Moon. Collisional elasticity effectively shifts the entire Roche zone outward, increasing the initial orbital radius required for material to be incorporated in a single body. Erosion will make the mass of the largest body which accretes at a given orbital radius, m_L, a stronger function of orbital radius, thus requiring steeper radial disk profiles than those shown in Fig. 6 for dm_L/da to be negative within the Roche zone.

VI. COMPARISON WITH IMPACT SIMULATION RESULTS

The natural trend is for bodies which accrete in the Roche zone to increase in mass with orbital radius, since inhibitive tidal effects diminish rapidly with orbital distance. The simplest means of averting this trend is to form the Moon from moonlets which accrete outside the Roche zone. For orbits exterior to the Roche zone, the innermost moonlet which forms will be the most massive in the disk as long as the radial surface density profile has $b \geq 2$, where $\sigma \propto (1/a)^b$. In this case, material initially having $a \gtrsim 3.5$–$4R_\oplus$ would be incorporated in the Moon. Material with $a < 3.5R_\oplus$ would need to eventually re-impact the Earth, either due to drag forces or to inward orbital evolution once a_{sync} has moved sufficiently outward due to the transfer of angular momentum from the Earth to the newborn Moon.

Table I shows that only a quarter of the published simulations place a lunar mass beyond the classical Roche limit for silicate, $2.9R_\oplus$. The closest candidates for ejecting $1M_M$ into orbits with $a > 3.5$–$4R_\oplus$ are the high angular momentum cases ($\sim$1.7–1.9 times the current Earth/Moon angular momentum) with an impactor mass of 1.2×10^{27} g (602 particles), or nearly twice the mass of Mars. Cameron (1986) has suggested that disk material will spread outward beyond the initial orbital radius of orbital insertion due to angular momentum transport processes in the disk, which, if it occurred prior to cooling and accretional growth, would help provide more material outside the Roche zone. Timescales for viscous spreading in the disk are extremely sensitive to the initial (and still unknown) physical state of ejected material (Thompson and Stevenson 1988). In addition, the long-term effect of viscous spreading is a net transfer of mass inward. The most direct way to provide enough material outside the Roche zone to form the Moon appears to be with a large impactor and a total impact angular momentum of about twice the current Earth/Moon system. This requires that a large amount of mass and angular momentum be eventually lost from the system. Although Cameron and Benz (1991) have postulated that such a "Giant Blowoff" would have occurred due to massive heating of the Earth and disk material, this remains a severe constraint.

In order to have the largest bodies in the disk accrete within the Roche zone, a very centrally condensed disk is required so that greater amounts of mass available for accretion in inner regions can offset increased tidal inhibition of growth. Figure 6 demonstrates that a very steep radial surface density profile is required to include material with $a < 3.5R_\oplus$, even for the limiting case of completely inelastic collisions. However, such steep profiles may be the natural result of giant impacts (Cameron 1994). Figure 11 is a plot of the radial density profiles resulting from three widely different types of impacts modeled by the Cameron *et al.* SPH simulation. Cameron (1994) has noted the common trend of a centrally condensed disk, which is relatively insensitive to the specifics of the impact event. Figure 12a is a plot of moonlets which accrete in a 1 or $2M_M$ disk having the Cameron (1994) "Case 6" density profile. The moonlets which form at 3.0–$3.8R_\oplus$ are all very close in mass and will occupy colliding orbits within and just exterior to the Roche zone, as shown in Fig. 12b. If these moonlets collide very inelastically and are able to accumulate all material with $a > 3.0R_\oplus$, they will form a body massive enough to overtake the exterior moonlets. The mass of the resulting moon is dependent on the radial dependence of the scale height in the disk.

VII. OTHER FORMATION SCENARIOS

There are several other means of incorporating all material in a protolunar disk exterior to synchronous orbit into a single Moon. These scenarios involve "seeding" accretional growth in the inner disk with massive objects derived from processes other than the collisional growth of silicate density material.

Large Intact Fragments

The most direct way to seed accretional growth in the inner disk is to begin with an initial distribution which contains one very large body with mass greater than m_0/μ_{crit}, where m_0 is the mass of the next largest body in the swarm. Such a body could theoretically accrete all surrounding material even within the Roche zone. For instance, a 500-km-radius body ejected intact into a low orbit could accumulate meter-sized bodies for all orbits with $a \gtrsim 2.5R_\oplus$. If this body were able to accrete all material within the Roche zone, it would be the most massive body in the disk for radial surface density profiles with $b \geq 2$. There could be several such fragment seeds located

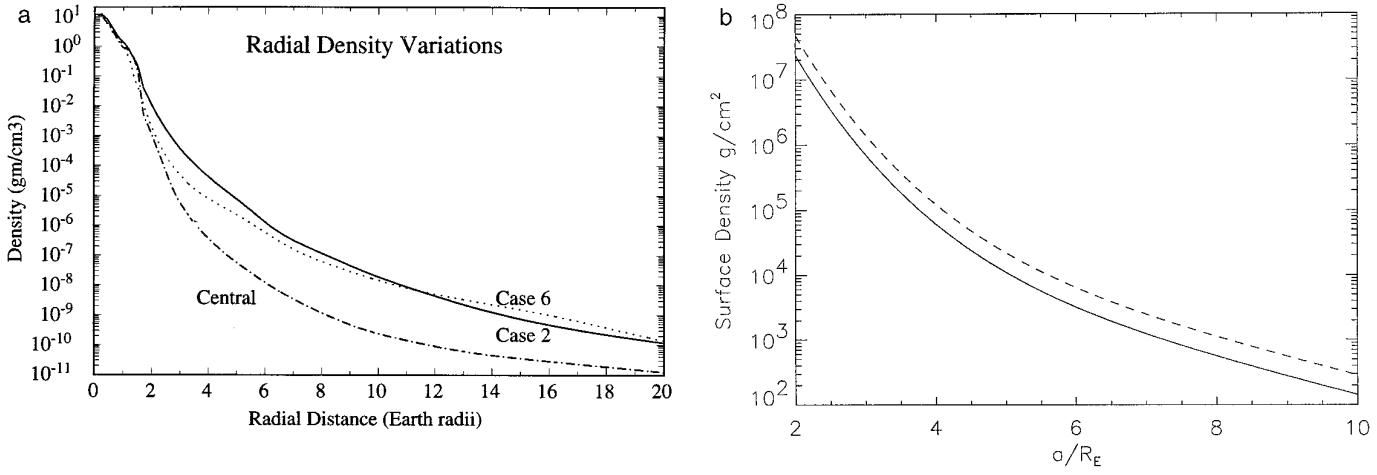

FIG. 11. (a) Radial density profiles from Cameron (1994). Case 2 was for the collision of two half-protoearths with an angular momentum 2.2 times the present system; Case 6 was for an impactor of mass 1.2×10^{27} g and angular momentum of 1.4 times the present system. The "Central" case was for an impact with zero angular momentum by a 1.2×10^{27} g body. (b) Surface density profiles for the Case 6 density profile for a 1 (solid) and 2 (dashed) lunar mass disk, assuming a uniform scale height in the disk.

at various regions in the disk, as long as the innermost fragment was also the largest.

The main difficulties with this scenario include allowing large objects to survive the impact event intact and accounting for the great difference in size required between the seeds and the rest of the ejected debris. In addition, the long phase of fragmentation that a protolunar disk would evolve through prior to accretional growth would likely yield power-law distributions in the disk regardless of initial size distributions. Power-law distributions of silicate density material would experience the accretional evolution patterns described in the previous sections.

Gravitational Instabilities

Formation of bodies in the protolunar disk through gravitational instability has been proposed by Thompson and Stevenson (1988). A hot gaseous disk has thermal velocities much too high to allow for collapse due to self-gravity. However, Thompson and Stevenson have noted that a two-phase, vapor/fluid disk has a much lower sound speed than a single phase disk due to the compressibility of a "foam" type mixture, and so may be gravitationally unstable at high temperatures.

Thompson and Stevenson model the protolunar disk as a two-phase medium, using Toomre's criterion for stability

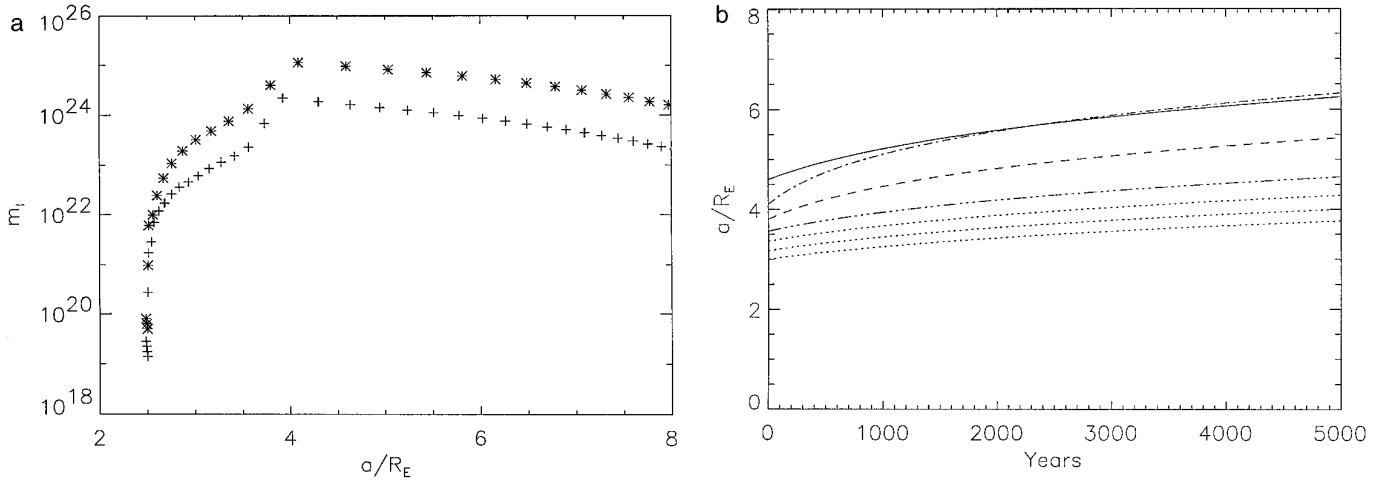

FIG. 12. (a) Distribution of moonlets which accrete from the Cameron (1994) Case 6 surface density profile. Here m_L is the mass of the largest body which accretes in each collisional zone. (b) The tidal orbital evolution paths for moonlets in (a).

of a think disk against radial perturbations to determine if the disk will fragment into mass "patches." There are several uncertainties associated with this analysis. First, it is unclear if the standard Toomre criterion can be aptly applied to a two-phase medium. In an equilibrium two-phase disk, a compressional wave could induce phase changes which would in turn alter the local compressibility of the medium and therefore the sound speed. The speed of sound in a two-phase medium might evolve drastically due to phase changes induced by compression during gravitational infall. In contrast, Toomre's criterion assumes an isothermal disk with a constant sound speed.

If the protolunar disk were to fragment due to gravitational instability, the mass patches formed would be stable only outside the classical Roche limit; interior to this they are sheared apart by tidal forces. Impact simulations (Cameron 1994) yield surface densities higher than those required for instability only for $a < 4R_\oplus$, and so there is a very narrow range of orbital radius over which the growth of mass concentrations due to instability could occur. In addition to high surface densities, instability requires a very specific range of vapor/fluid ratios and a disk scale height of only tens of kilometers. Whether or not the protolunar disk would ever pass through such a condensed foam phase is uncertain. If mass concentrations did form due to instability, the mass of patches predicted by Thompson and Stevenson increases with orbital radius, and so it is not obvious how a single Moon could result.

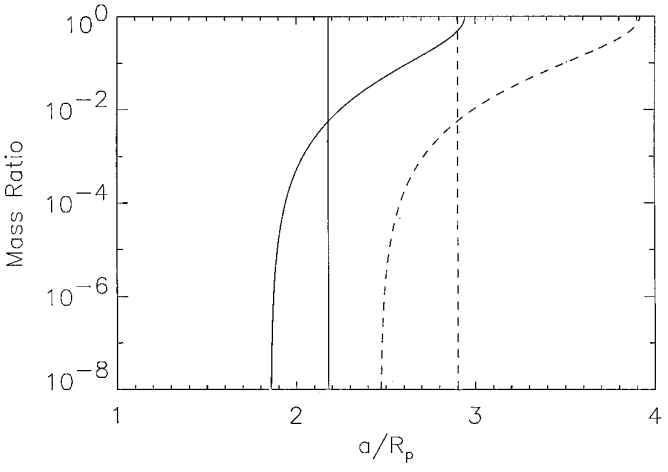

FIG. 13. The critical mass ratio curves for accretion of Fe (solid) and silicates (dashed). The respective classical Roche limits are indicated by vertical lines. Because of its high density (~7.8 g/cm^3), Fe can accrete efficiently at more inner orbital radii.

Fe Accretion in Inner Disk

We have thus far considered a protolunar disk with a uniform silicate-density composition. However, impact simulations (see Table I) often predict orbital injection of some iron from the core of the impactor. Metallic iron, with a density of more than twice that of typical silicates, can easily accrete at orbital radii interior to the Roche zone for silicate density material. Figure 13 ocmpares the critical mass ratio curve for accretion of silicate density material to that of Fe. Iron would accumulate efficiently for $a > 2.5R_\oplus$, and a massive enough Fe core formed in the inner disk could evolve outward and accumulate all exterior silicate material.

In a debris disk of solid or molten bodies, iron and silicate density materials would be well-mixed during the accretion process. However, if material ejected by a giant impact were substantially vaporized, metallic Fe would be one of the first elements to condense, and could accrete prior to the condensation of most lower-density materials. Figure 14 shows the condensation curves of solar composition material as a function of temperature and pressure (Lewis 1972). Fractionation of Fe from magnesium silicates in higher temperature regions of the inner solar nebula had been proposed to explain Mercury's anomalously high iron content in the so-called "equilibrium condensation hypothesis" (Lewis 1972). In that case, low solar nebular pressures (~10^{-3} bar) imply differences in condensation temperatures between Fe and silicates of not more than 100 K, which is insufficient to account for Fe/silicate fractionation in a collisional zone wide enough to form Mercury (Weidenschilling 1978). However, pressures in the inner protolunar disk would likely be much higher. Thompson and Stevenson (1988) predict mid-plane pressures for a vapor/fluid disk at $2R_\oplus$ of 0.1–1 bar for vertical disk heights ranging from $0.1R_\oplus$ to the midplane, respectively. The time for a disk one lunar mass disk of radius $3R_\oplus$ to cool from 1900 to 1700 K is (from Eq. (2)) approximately 1 year. Figure 15 shows the accretional evolution of a distribution of Fe at $2.6R_\oplus$. After 1 month, bodies initially 10 m in radius accrete to form bodies in the mass range 10^{21}–10^{23} g, and there is a 50% probability that all the mass has accumulated into a single body of mass 10^{23} g. Moonlets of these masses could easily sweep up exterior silicate material as they evolved outward and are significantly smaller than the upper limit on the mass of a lunar core from geophysical constraints ($\lesssim 4.4 \times 10^{24}$ g). Even much smaller iron bodies might help to incorporate some material from the inner protolunar disk.

VIII. CONCLUSIONS AND DISCUSSION

The final stage of the Giant-Impact scenario—accretion of a single, massive Moon from a centrally condensed protolunar disk—has not been well modeled. The analysis of accretional growth presented in Canup and Esposito (1995), as well as the character of all of the ring and satellite

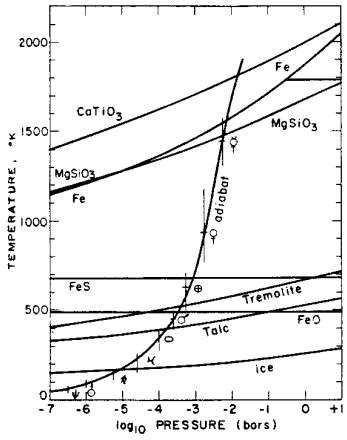

FIG. 14. The condensation curves for $CaTiO_3$ (a representative refractory mineral), Fe, $MgSiO_3$ (a magnesium silicate), and ice from solar composition material (from Lewis 1972). Additional lines indicate the appearance temperatures of FeS, tremolite (a hydrous calcium silicate), and talc (a hydrous magnesium silicate); the FeO line indicates the temperature at which Fe metal is wholly oxidized to FeO (as $FeSiO_3$ and Fe_2SiO_4). At high pressures likely in the inner protolunar disk, Fe would condense at temperatures several hundred degrees higher than silicates.

systems of the outer planets, predicts the formation of bodies which increase in mass with orbital radius for most initial disk conditions. This is in direct contrast to what is required for moonlets in the protolunar disk to evolve into colliding orbits to form a single Moon. This work has identified several classes of disk conditions which could yield a single Moon through a combination of accretion and tidal orbital evolution.

1. *Protolunar disks containing a lunar mass of material exterior to the Roche zone yield a single Moon for radial disk surface density profiles with $b \leq 2$, where $\sigma \propto (1/a)^b$.* Outside the Roche zone, accreted moonlets will decrease in mass with orbital radius if $b \geq 2$. For silicate density material and completely inelastic collisions, the outer edge of the Roche zone is at ~ 3.5–$4R_\oplus$; collisional elasticity moves this boundary outward. In this scenario, all mass interior to the outer edge of the Roche zone would eventually have to re-impact the Earth or be otherwise lost from the system. Simulations of giant impacts which are closest to satisfying this criterion describe large angular momentum (nearly twice that of the current system) impacts with the Earth by impactors nearly twice the mass of Mars (see Table I).

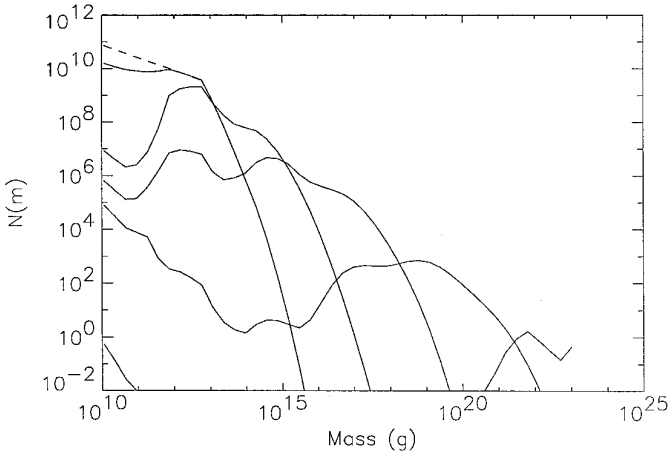

FIG. 15. The evolution of a mass distribution of Fe at $2.6R_\oplus$. The initial distribution is composed of 10- to 30-m-radius bodies; the final distribution at $t \sim 1$ month is composed of 10^{21}–10^{23} g bodies.

2. *Moonlets which accrete in the Roche zone may contribute to the Moon in an extremely centrally condensed protolunar disk. This requires a radial surface density profile with $b \gtrsim 10$ to exist throughout the accretional growth phase.* The inhibition of accretional growth by tidal forces within the Roche zone can be offset by having a much larger amount of mass available for accretion at smaller orbital radii. Surface density profiles produced by impact simulations typically have $b \gtrsim 8$ (Cameron 1994). However, the resolution of these simulations is insufficient to make firm predictions of disk structure. More importantly, such a steep gradient may be impossible to sustain against collisions and early rapid viscous spreading.

3. *Accretional growth in the inner disk may be "seeded" by bodies formed through processes other than collisional growth of silicates.* There are several possible seeding processes. The high density of Fe allows it to efficiently accrete at inner orbital radii, and formation of an iron core could seed accretional growth of silicates at 2.5–$3R_\oplus$. The difference in condensation temperatures ($\Delta T \sim 200$ K) between Fe and silicates could allow for Fe accretion prior to significant silicate condensation, assuming an initially vaporized disk. An iron core much less massive than the geophysical upper limits for the size of the lunar core would suffice to allow for incorporation of inner disk material into the Moon. Seeding of accretional growth could also occur if a fragments of mass $\sim 10^{22}$ g ($r \gtrsim 100$ km) or larger were ejected intact into low orbits, or if bodies formed in the inner disk due to gravitational instability. The latter requires a narrow range of disk temperature, physical phases, and densities.

Table II compares the conditions required for these three scenarios to yield a single lunar-sized Moon. With the impact simulation data published to date, no single scenario stands out as the most probable, although scenarios (2) (steep radial profile) and (3b) (seeding with instability) are the most physically restrictive.

The analysis presented in this paper has considered extreme conditions in order to determine the least restrictive criteria for inclusion of material with $a \lesssim 4R_\oplus$ into the

TABLE II
Requirements for Accretion of a Protolunar Disk into a Single Moon

Constraints	Scenario 1: Form Moon outside Roche zone	Scenario 2: Centrally-Condensed Disk	Scenario 3a: "Seeding" with Intact Fragment	Scenario 3b: "Seeding" with Gravitational Instabilities	Scenario 3c: "Seeding" with Fe core
Disk Structure	$\geq 1M_M$ with $a > 3.5\text{-}4\ R_E$	Very steep radial surface density profile (see below)	One fragment much more massive than all other material	$\sigma \sim 10^6$ g/cm^2 and a two-phase layer with scale height ~ 50 km (T & S 1988)	Iron in inner regions of vapor disk condenses first
Slope of Radial Surface Density Profile ("b")	$b \geq 2$	$b \geq 10$	$b \geq 2$	$b \geq 2$	$b \geq 2$
Mass and Angular Momentum of Impactor	$M_I > 10^{27}$ g with about twice the current system's angular momentum	Unknown	Unknown	Unknown	Unknown
Disk Evolution	All material with $a \lesssim 3.5\ R_E$ must re-impact Earth	Steep radial density gradient must be maintained throughout accretional growth. All material with $a < 2.6\ R_E$ must re-impact Earth	All material interior to radius of "seed" must re-impact Earth	All material with $a \lesssim 2.9\ R_E$ must re-impact Earth	All material with $a \lesssim 2.5\ R_E$ must re-impact Earth
Physical Phase of Disk Material	Unconstrained	Unconstrained	Intact solid or molten seed required	Two-phase vapor/fluid "foam" state	Vaporized disk material
Comments	Requires significant mass loss to rid excess angular momentum	Requires collisions to have $\varepsilon < .25$ (see Figure 10)	Fragment would need to be > 10^6 times more massive than other bodies to seed growth at $2.5R_E$	Instability-produced "patches" are stable outside $2.9\ R_E$	Fe core could accrete at $a \gtrsim 2.5\ R_E$

Note. Using the Canup and Esposito (1995) accretion model and assuming orbital evolution due to tidal interaction with the Earth; see text for details.

Moon. The assumption of completely inelastic collisional growth yields the innermost range of orbital radii over which tidal forces restrict accretional growth, as shown in Fig. 10. Inclusion of competing erosional processes would likely make the mass of moonlets which form in the Roche zone a stronger function of orbital radius than indicated in this analysis, since minimum collision velocities due to Keplerian shear are higher for inner orbits. In this case, an even steeper radial surface density profile would be required for scenario (2). Finally, it has been assumed that bodies with $\delta a \leq 3.5 R_{\rm Hill}$ will eventually accrete. The co-orbital satellites of Saturn offer at least one example of how this might not occur.

Forming the Moon from an impact-generated disk is a recent problem, and much work still needs to be done. Improved impact simulations are needed to provide more detailed information on initial disk conditions. The results of such simulations could distinguish between the formation scenarios outlined above, particularly if they more clearly constrain the initial physical state of ejected material, and/or determine if large, high-angular-momentum impactors can effectively place enough material into bound orbits beyond the Roche zone to form the Moon.

The viscous evolution of the protolunar disk depends strongly on both the radial surface density in the disk and on the exact nature (vapor, fluid, solid, or a combination

thereof) of the disk material. A turbulent gaseous disk may spread significantly prior to cooling and accretional growth, allowing some material to be placed in higher orbits. However, the net effect of viscous transport is a mass flux *inward,* and so is a relatively inefficient means of transporting a significant amount of material out of the Roche zone. Viscious spreading would also affect the radial density profile in the protolunar disk prior to accretional growth. In general, diffusive processes tend to remove pre-existing gradients. If viscous evolution in the disk lessened whatever radial density gradient existed immediately after disk formation, the requirement for the slope of the radial surface density in scenario (2) would be more extreme.

The final steps in lunar formation involve multiple moonlets accreting to form a single Moon. In this work we have assumed that moonlets whose orbits cross due to tidal evolution would accrete, and that it is likely that those whose orbits evolved within $3.5R_{\rm Hill}$ would also accrete. However, numerical simulations are necessary to assess the most likely outcomes as one satellite overtakes another. It is possible (especially for moonlets close in mass) that co-rotational horseshoe orbits or resonant configurations would be more probable than mutual accretion. In this case, explaining the formation of a single Moon from an impact-generated disk becomes even more difficult.

Although protosatellite disks around the outer planets have yielded systems of multiple moons, it is reasonable to expect that conditions and processes in an impact-generated disk should be somewhat unusual. Collisions among molten bodies in a hot protolunar disk might have been very nearly inelastic. A very steep radial surface density gradient may be the natural result of ejecting debris from an impact site into bound orbits by pressure gradients or gravitational torques. Heavy metals may have condensed from a hot disk prior to silicates, their rapid accretion at inner orbits (allowed for by their high densities) providing seeds for further accretional growth.

However, this work, whose parameters and assumptions have been chosen to maximize the likelihood of lunar accretion, has drastically limited the classes of disk candidates which could yield our single Moon. Our results raise some significant questions. Would inclusion of collisional elasticity and fragmentation preclude accretion in the Roche zone? Is it reasonable to postulate a Giant Impact with twice (or more) the current Earth/Moon angular momentum? Do moons which tidally evolve past one another necessarily accrete? What is the most likely initial radial distribution of material following an impact event, and how does this material evolve prior to cooling and accretional growth? The answers to these questions are crucial to the further evaluation of the ''Giant Impact'' scenario.

ACKNOWLEDGMENTS

We thank the members of the CU ''Ring Group''—Glen Stewart, Mihaly Horanyi, and Josh Colwell—for their many contributions to this work. Bill Hartmann, who got us interested in this problem in the first place, kindly provided us with unpublished material from his earlier work with Dominique Spaute, and offered helpful comments on this manuscript. Jay Melosh and an anonymous reviewer provided valuable suggestions. This work has been supported by NASA Grant NAGW-4373.

REFERENCES

Benz, W., W. L. Slattery, and A. G. W. Cameron 1986. The origin of the Moon and the single impact hypothesis I. *Icarus* **66,** 515–535.

Benz, W., W. L. Slattery, and A. G. W. Cameron 1987. The origin of the Moon and the single impact hypothesis II. *Icarus* **71,** 30–45.

Benz, W., A. G. W. Cameron, and H. J. Melosh 1989. The origin of the Moon and the single impact hypothesis III. *Icarus* **81,** 113–131.

Birn, J. 1973. On the stability of the Solar System. *Astron. Astrophys.* **24,** 283–293.

Burns, J. A. 1973. Where are the satellites of the inner planets? *Nat. Phys. Sci.* **242,** 23–25.

Burns, J. A. 1986. The evolution of satellite orbits. In *Satellites* (J. A. Burns and M. S. Matthews, Eds.), pp. 117–158. Univ. of Arizona Press, Tucson.

Cameron, A. G. W. 1986. The impact theory for origin of the Moon. In *Origin of the Moon,* pp. 609–616. Lunar Planet. Inst., Houston.

Cameron, A. G. W. 1994. Comparative results from giant impact studies. *Proc. Lunar Planet. Sci. Conf. 25th,* 215–216.

Cameron, A. G. W., and W. Benz 1991. The origin of the Moon and the single impact hypothesis IV. *Icarus* **92,** 204–216.

Cameron, A. G. W., and W. R. Ward 1976. The origin of the Moon. *Proc. Lunar Planet. Sci. Conf. 7th,* 120–122.

Canup, R. M., and L. W. Esposito 1995. Accretion in the Roche Zone: Co-existence of rings and ringmoons. *Icarus* **113,** 331–352.

Gladman, B. 1993. Dynamics of systems of two close planets. *Icarus* **106,** 247–263.

Greenberg, R., J. F. Wacker, W. K. Hartmann, and C. R. Chapman 1978. Planetesimals to planets: Numerical simulation of collisional evolution. *Icarus* **35,** 1–26.

Hartmann, W. K. 1978. Planet formation: Mechanism of early growth. *Icarus* **33,** 50–61.

Hartmann, W. K., and D. R. Davis 1975. Satellite-sized planetesimals and lunar origin. *Icarus* **24,** 504–515.

Kipp, M. E., and H. J. Melosh 1986. Short note: A preliminary numerical study of colliding planets. In *Origin of the Moon,* LPI, 643–648.

Kipp, M. E., and H. J. Melosh 1987. A numerical study of the giant impact origin of the Moon: The first half hour. *Proc. Lunar Planet. Sci. Conf. 28th,* 491–492.

Lewis, J. S. 1972. Metal/silicate fractionation in the Solar System. *Earth Planet. Sci. Lett.* **15,** 286–290.

Lissauer, J. J. 1995. On the diversity of plausible planetary systems (Urey Prize Lecture). *Icarus* **114,** 217–236.

Lissauer, J. J., and V. S. Safronov 1991. The random component of planetary rotation. *Icarus* **93,** 288–297.

Ohtsuki, K. 1993. Capture probability of colliding planetesimals: Dynamical constraints on the accretion of planets, satellites, and ring particles. *Icarus* **106,** 228–246.

Petit, J.-M., and M. Henon 1986. Satellite encounters. *Icarus* **66,** 536–555.

Ross, M. N., and G. Schubert 1989. Evolution of the lunar orbit with temperature and frequency dependent dissipation. *J. Geophys. Res.* **94,** 9533–9544.

Ruskol, E. L. 1973. On the model of the accumulation of the Moon compatible with the data on the composition and the age of lunar rocks. In *The Moon,* pp. 190–201. Reidel.

Ruskol, E. L. 1977. The Origin of the Moon. In *Cosmochemistry of the Moon and the Planets.* Academy of Sciences, Moscow, USSR.

Spaute, D., S. J. Weidenschilling, D. R. Davis, and F. Marzari 1991. Accretional evolution of a planetesimal swarm. I. A new simulation. *Icarus* **92,** 147–164.

Stewart, G. R., and G. W. Wetherill 1988. Evolution of planetesimal velocities. *Icarus* **74,** 542–553.

Stevenson, D. J. 1987. Origin of the Moon—The collision hypothesis. *Annu. Rev. Earth Planet. Sci.* **15,** 271–315.

Thompson, C., and D. J. Stevenson 1988. Gravitational instability in two-phase disks and the origin of the Moon. *Astrophys. J.* **333,** 452–481.

Weidenschilling, S. J. 1978. Iron/silicate fractionation and the origin of Mercury. *Icarus* **35,** 99–111.

Weidenschilling, S. J., C. R. Chapman, D. R. Davis, and R. Greenberg 1984. Ring particles: Collisional interactions and physical nature. In *Planetary Rings,* (R. Greenberg and A. Brahic, Eds.). pp. 367–415. Univ. of Arizona Press, Tucson.

Wetherill, G. W., and G. R. Stewart 1993. Formation of planetary embryos: Effects of fragmentation, low relative velocity, and independent variation of eccentricity and inclination. *Icarus* **106,** 190–209.